

FOURTEENTH EUROPEAN ROTORCRAFT FORUM

Paper No. 7

A NEW COMPUTATIONAL METHOD APPLIED TO ACCELERATION
POTENTIAL THEORY

J-J.COSTES - G.HARDY

OFFICE NATIONAL D'ETUDES ET DE RECHERCHES AEROSPATIALES
CHATILLON SOUS BAGNEUX , FRANCE

20-23 september, 1988
MILANO, ITALY

ASSOCIAZIONE INDUSTRIE AEROSPAZIALI
ASSOCIAZIONE ITALIANA DI AERONAUTICA ED ASTRONAUTICA

UNE NOUVELLE METHODE DE CALCUL APPLIQUEE A LA THEORIE DU POTENTIEL D'ACCELERATION

Résumé

Les méthodes intégrales sont en aérodynamique très adaptées à l'étude des phénomènes aéroélastiques complexes . Cependant les singularités qui interviennent dans ces méthodes doivent être traitées avec beaucoup de soin . Dans cet article , on donne une application de la théorie du potentiel d'accélération à l'hélicoptère . La pale est schématisée par des lignes portantes et une condition de glissement du fluide sur la pale est écrite en des points particuliers dits de collocation . Le traitement mathématique des singularités qui surviennent lorsque une ligne portante passe sur un point de collocation est donné en détail . La théorie a été validée par comparaison avec une expérience en soufflerie . Des calculs ont également été effectués pour le rotor de la Gazelle .

A NEW COMPUTATIONAL METHOD APPLIED TO ACCELERATION POTENTIAL THEORY

by J-J.Costes and G.Hardy

Office National d'Etudes et de Recherches Aérospatiales
BP 72. F - 92322 Châtillon Cedex , France

Abstract

In aerodynamics , integral methods are well suited for the study of complex aero-elastic problems . However the singularities of the functions which are integrated need to be treated very carefully . This paper shows an application of the acceleration potential theory for the helicopter . The blade is schematized by a set of lifting lines and a non separation condition of the flow from the blade surface is written on collocation points . The treatment of the mathematical singularities which occur when a lifting line passes on a collocation point is detailed . The theory has been validated by comparison with a wind tunnel test . Predictions were also made for the Gazelle helicopter rotor .

I INTRODUCTION

In recent years , the advent of fast and relatively inexpensive computers has allowed aerodynamicists to write CFD codes for helicopter rotors . These codes have various degrees of complexity (small disturbance potential , full potential , Euler codes ...) . Developed mainly for aeroelastic purposes , the method presented here is less sophisticated but fast (about 2 minutes on a CRAY-XMP computer) . It is based on the linear acceleration potential theory and cannot account for wake deformations or shocks.

II LINEAR THEORY

1. Acceleration and velocity potentials

The fluid is supposed perfect , compressible and unviscid , the perturbations are small and isentropic . Second order terms are neglected in the theory . The fluid acceleration is supposed derived from a potential ψ . It can be proved [1-2] that the acceleration potential created at a point P and at time τ by a moving doublet singularity is given by equation (1) .

$$\psi(P, \tau) = - \frac{\frac{d}{d\tau_0} [q_0 \vec{n}_0] \cdot P_0 \vec{P}}{4\pi a |P_0 P|^2 \left[1 - \frac{V_0 \cdot P_0 \vec{P}}{a |P_0 P|} \right]^2} \rightarrow \quad (1)$$

$$- q(\tau_0) \frac{[P_0 \vec{P} \cdot \vec{\gamma}_0][\vec{n}_0 \cdot P_0 \vec{P}] + (a^2 - V_0^2)(\vec{n}_0 \cdot P_0 \vec{P}) + [V_0 \cdot P_0 \vec{P} - a |P_0 P|][V_0 \cdot \vec{n}_0]}{4\pi a^2 |P_0 P|^3 \left[1 - \frac{V_0 \cdot P_0 \vec{P}}{a |P_0 P|} \right]^3}$$

where : q_0 is the doublet intensity
 \vec{n}_0 is the doublet direction
 P_0 is the position of the doublet
 V_0 is the doublet velocity
 $\vec{\gamma}_0$ is the doublet acceleration

All the variables with the subscript 0 are at time τ_0 .

The perturbation propagates in the fluid with a finite velocity a . The time τ at which the acceleration potential is given is related to the time τ_0 by the equation (2):

$$\tau - \tau_0 = \frac{|P_0P|}{a} \quad (2)$$

In fact we wish to compute the velocity potential at a time t and this can be done by integrating the acceleration potential of equation (1) over time. Moreover, for the case of a moving lifting surface another integration must be carried out over the surface. In the particular case of a helicopter, the large aspect ratio blade is replaced by a set of lifting lines. For simplification, only one lifting line is considered in the following theory, but the generalization to any number of lifting lines is simple. It has been proved in [3] that the velocity potential at a point P at time t is given by equation (3) where \vec{n}_0 , the doublet axis, is normal to the surface generated by the motion of the lifting line.

$$\begin{aligned} \phi(P, t) = & \int_{\text{lift. line}} \frac{-q(\tau_1) \vec{n}_0(\tau_1) \cdot \overrightarrow{P_0(\tau_1)P}}{4\pi a |P_0(\tau_1)P|^2 \left[1 - \frac{V_0(\tau_1) \cdot \overrightarrow{P_0(\tau_1)P}}{a |P_0(\tau_1)P|} \right]} d\sigma \rightarrow \\ & + \int_{\text{lift. line}} \int_{-\infty}^{\tau_1} \frac{-q_0(\tau_0) \cdot (\vec{n}_0(\tau_0) \cdot \overrightarrow{P_0(\tau_0)P})}{4\pi |P_0(\tau_0)P|^3} d\tau_0 d\sigma \end{aligned} \quad (3)$$

q_0, n_0, P_0 are also function of σ , this has been omitted in (3) for greater clarity.

The time τ_1 is a function of the lifting line curvilinear abscissa σ . Time τ_1 is defined as follow:

Let us consider a point P_0 on the lifting line at time τ_0 , the doublet associated with P_0 is at the position $P_0(\sigma, \tau_0)$. The perturbation induced into the fluid by the doublet propagates with velocity a and reaches the point P at time τ . If $\tau \leq t$, the point P_0 influences the point P . This condition defines a region of the wake which influences P at time t . The limit of this region is the line $P_0[\sigma, \tau_1(\sigma)]$, which is determined by the non-linear equation (4).

$$a \cdot (t - \tau_1[\sigma]) = |PP_0[\sigma, \tau_1(\sigma)]| \quad (4)$$

When the fluid is incompressible, the velocity of sound becomes infinite and from (4), $\tau_1 = t$. Furthermore the first integral in (3) is equal to zero. For a compressible fluid, the potential ϕ is equal to an incompressible term integrated over only one part of the wake (second integral in equation (3)). This integration is completed by a curvilinear integral along the boundary represented by the line having the equation $P_0[\sigma, \tau_1(\sigma)]$ (first integral in equation (3)).

The derivation of ϕ with respect to the geometrical coordinates of P determines the velocity induced in space by the moving lifting line. For the computation of the lifting forces, one only needs to know the velocity component normal to the wake when the point P is exactly on the wake.

2. Application to the helicopter rotor in forward flight

Let us first consider the simplest case where the blade is schematized by a single straight lifting line. Neither precone nor blade movements in flap or lag are taken into account. The rotor center of rotation is supposed to be located on the lifting line. For the blade i , the azimuthal angle at time τ is given by the equation:

$$\Theta_i(\tau) = \Omega \tau + \theta_i \quad (5)$$

where $\theta_{i+1} - \theta_i = \frac{2\pi}{n}$ and n is the number of rotor blades .

In an absolute reference frame , the geometrical coordinates at time τ of a point P belonging to the lifting line and located at a distance r from the center of rotation are given by (see figure [1]) :

$$P(r, \tau) = \begin{cases} X = r \cos \Theta_i - V_X \tau \\ Y = r \sin \Theta_i \\ Z = V_Z \tau \end{cases} \quad (6)$$

where V_X and V_Z are coordinate components of the rotor velocity .

The wake of the blade is taken as the surface generated by the motion of the lifting line . A point $P(r, \tau)$ is selected on the wake of blade i , the normal \vec{n} to the wake is determined and a point P' is taken on this normal at a height h above the wake . The computation of the potential induced at the point P' by the wake of blade j is carried out by means of equation (3) . Once the potential has been found , it is differentiated with respect to h and the limit as h tends to zero is computed to obtain the induced velocity . The first integral in equation (3) is a simple curvilinear integral which never becomes singular . Its derivative may be obtained by a numerical computation which will not be detailed in this paper . The second integral in equation (3) gives a potential ϕ_2 and an induced velocity v_2 .

$$\begin{aligned} \lim_{h \rightarrow 0} \frac{\partial \phi_2}{\partial h} = v_2 = & - \frac{1}{4\pi} \int_{R_0}^{R_1} \int_{-\infty}^{\tau_1(r_0)} q(r_0, \tau_0) \frac{N_1}{U_{j0} U_i D^{3/2}} dr_0 d\tau_0 \quad \rightarrow \\ & - \frac{1}{4\pi} \int_{R_0}^{R_1} \int_{-\infty}^{\tau_1(r_0)} q(r_0, \tau_0) \left[\frac{-3V_Z^2}{U_{j0} U_i} \right] \frac{N_2}{D^{5/2}} dr_0 d\tau_0 \quad \rightarrow \\ & - \frac{1}{4\pi} \int_{R_0}^{R_1} \lim_{h \rightarrow 0} \left[q(r_0, \tau_1) \frac{\vec{n}_{0P} \cdot \vec{P}_0 P(r_0, \tau_1)}{|PP_0|^3} \cdot \frac{\partial \tau_1}{\partial h} \right] dr_0 \end{aligned} \quad (7)$$

where U_{j0} , U_i , D , N_1 et N_2 are given by :

$$U_{j0} = \left[V_X^2 + (r_0 \Omega + V_X \sin \Theta_{j0})^2 \right]^{1/2} \quad (8)$$

$$U_i = \left[V_X^2 + (r \Omega + V_X \sin \Theta_i)^2 \right]^{1/2} \quad (9)$$

$$D = r^2 + r_0^2 + (\tau - \tau_0)^2 (V_X^2 + V_Z^2) - 2rr_0 \cos(\Theta_{j0} - \Theta_i) + 2V_X(\tau - \tau_0)(r_0 \cos \Theta_{j0} - r \cos \Theta_i) \quad (10)$$

$$N_1 = V_Z^2 \cos(\Theta_{j0} - \Theta_i) + (r_0 \Omega + V_X \sin \Theta_{j0})(r \Omega + V_X \sin \Theta_i) \quad (11)$$

$$N_2 = rr_0 \Omega^2 (\tau - \tau_0)^2 + (r^2 + r_0^2) \Omega (\tau - \tau_0) \sin(\Theta_{j0} - \Theta_i) + rr_0 \sin^2(\Theta_{j0} - \Theta_i) \quad (12)$$

In equations (8 to 12) we have $\Theta_i = \Theta_i(\tau)$ and $\Theta_{j0} = \Theta_j(\tau_0)$.

The third integral in equation (7) is curvilinear and its denominator is always different from zero . Because of these two particularities it is readily computable numerically . On the other hand , the two surface integrals in equation (7) may become singular because D , which represents the square of the distance between the point P and the point $P_0(r_0, \tau_0)$, may

become equal to zero when P and P_0 belong to the same blade wake . The numerical evaluation of these two integrals will now be shown .

2.1. Integration over time in the non singular case

In this case the denominator D never becomes equal to zero when time τ_0 varies from $-\infty$ to τ_1 . We must look for a numerical method of integration that is fast and sufficiently accurate . For the particular case of a wing moving with a uniform velocity many methods have been devised [4-9] . That due to Desmarais [6] is particularly well known . It approximates the function to be integrated (the kernel) by a set of exponentials . For the particular case of the helicopter in forward flight , Desmarais' method does not apply . Furthermore the advent of modern computers based on parallel processing principles makes the approximating of the kernel by a set of not truly elementary functions less attractive. It may be more advantageous to evaluate repeatedly the kernel directly . Let us consider the functions U_{j0} , U_i , D , N_1 , N_2 , when r_0 is held fixed and τ_0 varies from $-\infty$ to τ_1 . N_2 and the denominator D are polynomial functions of $(\tau-\tau_0)$. As τ_0 tends toward $-\infty$, U_{j0} , U_i and N_1 remain bounded and D tends toward infinity like $(\tau-\tau_0)^2$. This ensures the convergence of the first integral in (7) . For the second integral in (7) the convergence arises from the fact that $D^{5/2}$ increases more rapidly than N_2 as τ tends towards $-\infty$. In the numerical evaluation of these two integrals , polynomial terms are computed by simple products and are no problem . Unfortunately U_{j0} , U_i , D , N_1 and N_2 also contain sine and cosine terms of the variable τ_0 . Obviously the number of calculations of the sines and cosines should be minimized . Taking r_0 as constant and omitting it in the following equations for more clarity , this minimization can be done in the following manner :

$$\int_{-\infty}^{\tau_1} \frac{q(\tau_0)N_1(\tau_0)}{U_{j0}(\tau_0)U_i(\tau_0)[D(\tau_0)]^{3/2}} d\tau_0 = \int_{\tau_1 - \frac{2\pi}{\Omega}}^{\tau_1} S_1(\tau_0) d\tau_0 \quad (13)$$

$$\text{With } S_1(\tau_0) = \frac{q(\tau_0)N_1(\tau_0)}{U_{j0}(\tau_0)U_i(\tau_0)} \sum_{k=0}^{+\infty} \frac{1}{\left[D\left(\tau_0 - \frac{2\pi k}{\Omega}\right) \right]^{3/2}} \quad (14)$$

For the second integral in (7) the same method applies with S_2 taken as :

$$S_2(\tau_0) = q(\tau_0) \left[\frac{-3V_Z^2}{U_{j0}U_i} \right] \sum_{k=0}^{+\infty} \frac{N_2\left(\tau_0 - \frac{2\pi k}{\Omega}\right)}{\left[D\left(\tau_0 - \frac{2\pi k}{\Omega}\right) \right]^{5/2}} \quad (15)$$

After some manipulation S_1 and S_2 can be obtained by a combination of the 4 series s_1 , s_2 , s_3 , s_4 below :

$$s_1(\tau_0) = \sum_{k=0}^{+\infty} \frac{1}{\left[1 + \left[\rho \cdot (\theta_0 + 2k\pi) + c \right]^2 \right]^{3/2}} \quad (16)$$

$$s_2(\tau_0) = \sum_{k=0}^{+\infty} \frac{1}{\left[1 + \left[\rho \cdot (\theta_0 + 2k\pi) + c \right]^2 \right]^{5/2}}$$

$$s_3(\tau_0) = \sum_{k=0}^{+\infty} \frac{\theta_0 + 2k\pi}{\left[1 + \left[\rho \cdot (\theta_0 + 2k\pi) + c\right]^2\right]^{5/2}}$$

$$s_4(\tau_0) = \sum_{k=0}^{+\infty} \frac{(\theta_0 + 2k\pi)^2}{\left[1 + \left[\rho \cdot (\theta_0 + 2k\pi) + c\right]^2\right]^{5/2}}$$

These four series depend on the 3 parameters θ_0 , ρ and c . The parameter θ_0 is an angle which is greater than 0 and less than 2π radians. The parameters ρ and c are functions of the coefficients V_X , V_Z , Ω , r , r_0 which are given by the rotor flight characteristics and by the positions of the points P and P_0 . The series have been studied for the following range of the parameters :

$$0 \leq \theta_0 \leq 2\pi$$

$$10^{-4} \leq \rho \leq 10^{+4}$$

$$0 \leq |c| \leq 10^{+4}$$

The order of magnitude of ρ and c are :

$$\rho \approx \lambda \cdot \frac{(V_X^2 + V_Z^2)^{1/2}}{|V_Z|} \quad c \approx \frac{V_X}{V_Z} \quad \text{with} \quad \lambda = \frac{(V_X^2 + V_Z^2)^{1/2}}{\Omega r}$$

λ is the advance ratio computed for the radial distance r of the point P . It should be noted that the particular case of $V_Z=0$ is not covered by the numerical method presented here. In fact the case $V_Z=0$, where the wakes of the blades are supposed to remain in the plane of the rotor disk, is mathematically extremely difficult and can be ignored in most engineering applications. Even for the case of the hovering rotor, the blade wakes are carried downward by the flow which exist across the rotor disk. However, in this case the wake deformations, which cannot be included in this theory, are likely to introduce large errors especially when V_Z is small or negative.

s_1 , s_2 , s_3 , s_4 are determined by one of the four following methods according to the values of ρ and c (see figure [2]) :

Method 1. The series are replaced by integrals from zero to infinity over the variable k . The analytical value of the integral is known but it can also be computed by the trapezium formula :

$$s = \sum_{k=0}^{+\infty} s(k) \approx -\frac{1}{2}s(0) + \int_0^{+\infty} s(k) dk$$

This relation gives an approximate value for the series.

Method 2. A number N is selected. The series is divided into two parts :

$$s = \sum_{k=0}^{k=N} s(k) + \sum_{k=N+1}^{\infty} s(k)$$

The second series is computed by means of method 1. For the first series, $s(k)$ is determined for 100 equally spaced values of k ($N = 100p$). The variation of $s(k)$ is supposed linear between to adjacent values of k .

Method 3. It is the same method as method 2 except that 1000 values of k are taken between 0 and N ($N = 1000p$).

Method 4 . For some particular combinations of the parameters ρ and c , the linear interpolation is not sufficient . Following the ideas applied in the auto-adaptive routines used in numerical integrations [10] , that is to say the successive division of the original interval and polynomial approximations , a special method of integration has been devised . Between $k=N_1$ and $k=N_2$, $s(k)$ is approximated by a polynomial of the 8th degree . With this assumption the sum $s(N_1, N_2) = \sum_{k=N_1}^{k=N_2} s(k)$ is calculated and then compared to the more accurate value obtained by cutting the original interval $[N_1 N_2]$ into two equal sub-intervals and calculating each partial sum by the same process . If the two results agree within some prescribed limit the computations are halted and if not the process is repeated for each sub-interval .

Remark 1 . It has been shown numerically that the parameter θ_0 is not a determining factor in the choice of the method of summation .

Remark 2 . Extensive computations have been carried out to compare the approximate evaluation of the series s_1, s_2, s_3, s_4 with values obtained by direct summation . In every case the error has been found to be inferior to $3 \cdot 10^{-5}$. So far no attempt has been made to optimize the number of points in methods 2 and 3 . The approach employed in method 4 using a linear approximation of $s(k)$ is possible and perhaps faster .

Remark 3 . The calculation of the sums of the 4 series s is the only part of the computer code that has been vectorised in the version used on the CRAY-XMP .

2.2. Integration over time in the singular case

In the singular case the points P and P_0 belong to the same blade wake ($i=j$) . For $\tau=\tau_0$, D tends toward zero as r_0 tends toward r . For the first integral in (7) let us define J_1 as :

$$J_1(r_0) = \int_{-\infty}^{\tau_1(r_0)} q(r_0, \tau_0) \frac{N_1}{U_{j_0} U_i D^{3/2}} d\tau_0 \quad (17)$$

For $\tau_0 = \tau$ and $r_0 = r$; N_1 , U_{i_0} , U_i are bounded and different from zero . Thus $J_1(r_0)$ becomes singular as r_0 tends toward r . Let us consider the product $(r_0 - r)^\alpha J_1(r_0)$ where $\alpha > 0$. It may be written as :

$$(r_0 - r)^\alpha J_1(r_0) = (r_0 - r)^\alpha \int_{\tau+\Delta\tau}^{\tau_1(r_0)} q \frac{N_1}{U_{j_0} U_i D^{3/2}} d\tau_0 \rightarrow \quad (18)$$

$$+ (r_0 - r)^\alpha \int_{\tau-\Delta\tau}^{\tau+\Delta\tau} q \frac{N_1}{U_{j_0} U_i D^{3/2}} d\tau_0 + (r_0 - r)^\alpha \int_{-\infty}^{\tau-\Delta\tau} q \frac{N_1}{U_{j_0} U_i D^{3/2}} d\tau_0$$

As r_0 tends toward r , the first and the third integrals in (18) are not singular and their contribution to $(r_0 - r)^\alpha J_1$ can be neglected , due to the fact that they are multiplied by $(r_0 - r)^\alpha$. Thus :

$$\lim_{r_0 \rightarrow r} (r_0 - r)^\alpha J_1(r_0) = \lim_{r_0 \rightarrow r} (r_0 - r)^\alpha \int_{\tau - \Delta\tau}^{\tau + \Delta\tau} q \frac{N_1}{U_{j_0} U_i D^{3/2}} d\tau_0 \quad (19)$$

This is true even if $\Delta\tau$ is small and therefore the integral in (19) can be studied by limited expansion. After lengthy developments, one can prove that $(r_0 - r)^\alpha J_1(r_0)$ has a finite value A_0 for $\alpha = 2$. The process may then be repeated:

$$\lim_{r_0 \rightarrow r} (r_0 - r) \left[J_1(r_0) - \frac{A_0}{(r_0 - r)^2} \right] = A_1$$

Thus
$$\lim_{r_0 \rightarrow r} J_1(r_0) = \frac{A_0}{(r_0 - r)^2} + \frac{A_1}{(r_0 - r)} + \dots \quad (20)$$

Remark 1. The above analysis is not complete, it overlooks any logarithmic singularity. Nevertheless, the contribution of a logarithmic singularity to J_1 would be small compared to the contribution of the two terms A_0 and A_1 and has thus been neglected.

Remark 2. A_0 and A_1 are determined analytically and therefore are known with great precision.

For the second integral in (7), let us define J_2 as:

$$J_2(r_0) = \int_{-\infty}^{\tau_1(r_0)} q(r_0, \tau_0) \left[\frac{-3V_z^2}{U_{j_0} U_i} \right] \frac{N_2}{D^{5/2}} d\tau_0 \quad (21)$$

For $\tau = \tau_0$ and $r_0 = r$, both N_2 and D are equal to zero but the integral J_2 is not singular. This can be proved by a limited expansion of the summed expression in J_2 . As r_0 tends towards r , the limit of J_2 is finite but it can only be determined by a numerical integration over the whole interval $[-\infty, \tau_1]$ which includes τ . In fact, it is unnecessary to compute J_2 for $r_0 = r$ because this can be obtained by the method of the preceding paragraph for values of r_0 very close to r .

$r : \left[\left| 1 - \frac{r_0}{r} \right| \leq 0.0001 \right]$. This determines J_2 with sufficient accuracy because the participation of J_2 in equation (7) is small compared to that of J_1 .

2.3. Integration along the blade span

As it has been shown above, J_1 is singular when r_0 tends toward r . The first integral in (7) must be taken as a Cauchy principal part integral, that is to say an original integral function must be found analytically and the value of the integral is given as the difference between the values of this function evaluated for $r_0 = R_0$ and $r_0 = R_1$. In the general case the original integral function is unknown. The idea is then to extract the singularity and to integrate numerically over the interval $[R_0, R_1]$. The Cauchy principal part of the singularity will then be added to the numerical result. The details of the method are given below:

$J_1(r_0)$ is approximated by the series K_1 .

$$J_1(r_0) \approx K_1(r_0) = \frac{1}{(r_0 - r)^2} \left[A_0 + (r_0 - r)A_1 + \dots + (r_0 - r)^n A_n \right] \quad (22)$$

The coefficients A_0 and A_1 have already been determined in (2.2), the remaining coefficients $A_2 \dots A_n$ may be chosen such that the relation (22) is verified for some selected values of the radial distance r_0 . For example with $n=3$ the relation (22) may be exact for $r_0=r \pm \Delta r$. The difference J_1-K_1 is not singular and may be integrated numerically over $[R_0, R_1]$. To avoid numerical problems, J_1-K_1 is assumed to be equal to zero in the interval $[r-\Delta r, r+\Delta r]$. Thus we have:

$$\oint_{R_0}^{R_1} J_1(r_0) dr_0 \approx \left[\frac{-A_0}{(r_0-r)} + A_1 \text{Log} |r_0-r| + A_2(r_0-r) + \frac{A_3}{2}(r_0-r)^2 \right]_{R_0}^{R_1} \rightarrow (23)$$

$$+ \int_{R_0}^{r-\Delta r} (J_1-K) dr_0 + \int_{r+\Delta r}^{R_1} (J_1-K) dr_0$$

A very important question is the accuracy obtained in the evaluation of the Cauchy integral in equation (23).

Let us consider the two integrals of equation (23), these integrals must be evaluated numerically. If r_0 is close to $r \pm \Delta r$ the function J_1-K has the same order of magnitude as $[1/\Delta r]^2$ which is very large when Δr is small. In the numerical computations $(r_0-r)^2 J_1(r_0)$ is evaluated instead of J_1 because the product of J_1 by $(r_0-r)^2$ is not singular when r_0 tends toward r . As $(r_0-r)^2 J_1(r_0)$ is a result of a complicated numerical process, its accuracy is likely to be poor (typically the relative error is equal to $3 \cdot 10^{-4}$). The error is multiplied by $[1/\Delta r]^2$ which has catastrophic effects when Δr is small. The above analysis shows that Δr must be chosen as large as possible for a good evaluation of the two integrals in equation (23).

In the interval $[r-\Delta r, r+\Delta r]$, J_1 is represented by the series K_1 with only four terms in the example chosen in writing equation (23). The series K_1 must represent very accurately the function J_1 over the whole interval $[r-\Delta r, r+\Delta r]$ and for this reason Δr must not be too large. The value of Δr must then be a compromise between two contradictory requirements. How this compromise should be made is not entirely understood at present. One possible solution is given below:

- 1- A large value of Δr is chosen.
- 2- The function $(r_0-r)^2 J_1(r_0)$ is numerically evaluated for $r_0 = r \pm \Delta r$.
- 3- The second degree polynomial $G(r_0)$ equal to A_0 for $r_0 = r$ and to $(r_0-r)^2 J_1(r_0)$ for $r_0 = r \pm \Delta r$ is determined.
- 4- The derivative of G is computed and its value for $r_0 = r$ is compared to the theoretical value of A_1 . If the difference between both values is considered negligible, then the value of Δr is retained. Otherwise Δr is halved and the whole process is repeated again, starting from step 2.

3. Determination of the aerodynamic forces on the rotor disk.

In the preceding paragraph we have shown how to calculate the velocity induced at some selected point on the lifting line path. This will now be used to determine the aerodynamic forces on the rotor disk.

The lifting force by unit length, $F(r_0, \tau_0)$, along the lifting line is related to the doublet intensity by the equation :

$$q(r_0, \tau_0) = - \frac{F(r_0, \tau_0)}{\rho_0} \quad (24)$$

where ρ_0 is the density of the undisturbed fluid .

$F(r_0, \tau_0)$ is decomposed in a set of polynomials for the radial variable r_0 and in a Fourier series for the time variable τ_0 .

$$F(r_0, \tau_0) = \sum_{i=1}^N X_i P_i(r_0) + \sum_{i=1}^N \sum_{j=1}^M Y_{ij} P_i(r_0) \cos j\Theta(\tau_0) \rightarrow \quad (25)$$

$$+ \sum_{i=1}^N \sum_{j=1}^M Z_{ij} P_i(r_0) \sin j\Theta(\tau_0)$$

In equation (25) , the polynomials $P_i(r_0)$ may be chosen as Legendre's polynomials, but in some of the applications presented in this paper , Jacobi's polynomials have also been used . These polynomials are orthogonal over the interval $[R_0, R_1]$ with a weighting function equal to 1 as for the Legendre polynomials , but the additional condition that they are equal to zero for $r_0=R_0$ is imposed . The velocity induced in the fluid by each of the functions $P_i(r_0)$, $P_i(r_0)\cos j\Theta(\tau_0)$, $P_i(r_0)\sin j\Theta(\tau_0)$ is computed for $N \cdot (2M+1)$ points carefully selected on the rotor disk . For each point , a non separation condition of the flow from the helicopter blade is written . This determines the value of the unknown coefficients X_i, Y_{ij}, Z_{ij} if the blade movement is known . It is now necessary to specify the positions of the collocation points on the helicopter blade . Starting from the azimuthal position $\Theta=0$, $2M+1$ equally spaced azimuths are selected and each is the azimuth of N collocation points . In the numerical applications presented below , the rotor blades are rectangular and the feathering axis is located at the quarter chord position . The feathering axis is assumed to generate the blade wake . In the case of the Jacobi polynomials $J(y)$, let us call y_i the values of y which put the polynomial of degree $N+1$ to zero. One of these values is equal to R_0 and is not considered . The remaining N y_i are on the interval $]R_0, R_1[$ (limits excluded) , and are used for the definition of the spanwise positions of the collocation points . In the acceleration potential theory , 2D steady analysis as well as empirical evidence from the 3D unsteady case suggest placing the collocation points on a line located at the third quarter chord position (when there is only one lifting line) . Now , on this line , two possibilities have been considered for the spanwise position of the collocation points :

- 1- The spanwise coordinates of the collocation points are equal to the y_i and , therefore do not depend on the azimuthal angle Θ .
- 2- Let us call Q_i the point on the quarter chord line at the spanwise coordinate y_i and P_i the collocation point that will also be determined by y_i . We want the spanwise component of the local flow velocity to influence the position of the collocation point P_i . This is done by allowing the collocation point P_i to position itself to leeward of the point Q_i while still remaining on the third quarter chord line . The spanwise coordinate of the point P_i now depends on the azimuthal angle Θ .

III NUMERICAL APPLICATIONS

Though the development of this new computational method for the acceleration potential theory is far from complete , some applications and comparisons with

experimental results have already been done . We first made computations for the incompressible case with a Prandtl correction for the non separation condition of the flow. These assumptions give a simpler program where some features such as the choice of Δr (see : II-2.3) are more easily investigated . A more complete code for compressible flow is also under development . It is possible with this code to use more than one lifting line to schematize the blade . One preliminary result has been obtained with two lifting lines .

As we are mainly concerned with the computation of the aerodynamic forces , in all the following applications the blade movement is supposed known and given by experiment or other codes . The full aeroelastic problem will be addressed later using a method devised by Tran [11] . His method can couple any aerodynamic model with elastic properties of the blades .

For our comparisons , we first used an early (1970) wind tunnel test to validate the codes , and then an application was attempted for a flight test case of the SA 349 GV Gazelle helicopter .

1. Validation of the codes

In 1970 a series of tests was carried out in the S1 wind tunnel in Modane on a rotor model having 3 rectangular blades . The lifting part of the blades was situated between the two radial positions $R_0=0.473 m$ and $R_1=2.075 m$. The chordwidth was $c=0.21 m$, and the profile was a NACA0012 along the whole blade span . With these dimensions , the glass fiber blades were very rigid , and any blade deformation such as bending or torsion could be neglected . The rotor had flap and lag hinges but there was no cyclic pitch . During the test , the blade flap and lag movements were recorded . The rotational speed of the rotor was about 96 rd/s which gave a velocity at the blade tip of about 200 m/s . There was no fuselage and the model design was such that its flight characteristics be close to those of actual helicopters of that time , though with purer aerodynamics, and the rotor attitude and blade movements be well defined . Four sections at radial distances $R/R_1=0.952$, 0.855 , 0.71 , 0.52 were instrumented with 10 differential pressure transducers . During the tests , the lift force per unit length was recorded , but there were not enough transducers for a reliable measurement of the moments and thus they are not available .

For the comparison between theory and experiment which will be presented below , a case with an advance ratio of 0.3 has been selected . The rotor was not heavily loaded , $C_T/\sigma \approx 0.1$, and thus the non linear aerodynamic effects on the retreating blade were probably small . The tip path plane angle , $\alpha_D=7.53^\circ$, was rather large but still representative of an actual flight case . The inputs for the computations were the experimental collective pitch angle and the recorded blade movement . No attempt was made to adjust the inputs and the comparisons given are for the lift per unit length (normalized by the chord \times static pressure product) . Though this case is not too difficult , the comparison between theory and experiment is still meaningful .

For the computations , 5 Jacobi polynomials and 6 harmonics were considered . The blade was schematized by a single lifting line at the quarter chord and the collocation points positions were varied with the azimuthal angle . The computer time required was about 2mn on a CRAY-XMP . Figure [3] shows the results obtained with an incompressible flow and a Prandtl correction for the non separation condition . The same figure also gives the results when the compressibility of the air is correctly included into the theory . These theoretical results compare very well with the experiment . The discrepancies are somewhat larger at the blade tip section ($R/R_1=0.952$) but the results remain very satisfactory , especially if one notes that they are obtain with a single lifting line blade model .

2. Application to the Gazelle helicopter

A series of flight tests has recently been completed with a Gazelle helicopter . The 3 blades of the rotor have a rectangular plan form and an OA 209 profile along the whole span . During the flights, pressures were measured on 3 instrumented blade sections . The blade movements were not recorded at the same time as the pressures but during another flight campaign . The measured blade collective and cyclic pitch were inaccurate because of the elasticity of the control system . Furthermore , our computations are at present restricted to the case of a hinged rotor with rigid blades . For the comparisons between theory and experiment , a flight case with a helicopter forward speed of 290 km/h was selected . The necessary inputs for the computations were obtained by using an earlier computer code [12-13] where the collective and cyclic pitch were trimmed to obtain the required lift and forward forces of the rotor . The lift is given as the aircraft gross weight , but the forward force which counteracts the total aircraft drag has been extrapolated from wind tunnel measurements by the Aerospatiale .

In the computations 5 Legendre polynomials and 6 harmonics were used . The results are given in figures [4 to 7] . For a high advance ratio flight case , we hope to improve the classical lifting line results by optimizing the positions of the collocation points as a function of the blade azimuthal angle . It is for this reason that the method of optimized collocation points is used here , even though in the case of the moderate advance ratio of the test ($\mu=0.356$) , the effect of the variation of the position of these points is not very significant (see figure [6]) .

The comparison between theory and experiment is given in figure [4] for the lift coefficient C_L . Though at first the comparison may seem good , an important phase shift is obvious between the theoretical and the experimental curves for the advancing blade at about 90° azimuthal angle . This phase shift can be seen more clearly in figure [5] where the lift coefficient C_L is multiplied by the square of the local Mach number . This Mach number M is derived from the normal component of the blade velocity . The product $C_L . M^2$ is a kind of normalized lift per unit length . The error on the section located at the radial position $R/R_1=0.88$ is particularly large . As shown in figure [6] the discrepancies cannot be explained by changes in the positions of the collocation points which , as expected , have no effect at 90° and 270° azimuthal angles . We have also attempted to remove some of the simplifications in the theory . As explained in II-2 , the blade wake is approximated by the surface generated by the movement of the blade quarter chord line . The movement of the quarter chord line is itself simplified and does not take into account the lateral tilt of the rotor plane . Though the complete blade movement is taken into account for the non separation condition written for each collocation point , it is necessary to know the effect of the wake simplification . Following the method given in II-2 , the complete equations have been derived . It has been found that the integration can still be done by using the four series $s_1(\tau_0)$, $s_2(\tau_0)$, $s_3(\tau_0)$, $s_4(\tau_0)$ given in II-2.1 . Thus the theory given in II can still be used with only a few modifications of the computer code . The results which were obtained with an exaggerated lateral tilt (5°) of the rotor tip path plane differ only very slightly from the ones shown in figures [4 and 5] and are therefore not presented here .

We have also tried to increase the number of lifting lines . Though the general theory remains unchanged , many details must be modified , in particular the definition of the aerodynamic forces along the blade span in equation (25) . The wake of the blade is still defined by the movement of the quarter chord line , but the lifting lines must now be projected on the wake . This has far reaching consequences on the computer code . The code is still in the development stage but results have already been obtained with 2 lifting lines . These are given in figure [7] for the lift coefficient C_L . The results with one or two lifting lines do

not differ much , and the main differences occur at the 270° azimuthal angle where they have very little effect on the lift .

The phase shift between the theoretical and experimental lift curves , illustrated by figure [5] , remains unexplained. The large torsion (1°) measured at the blade tip during the experiment may explain some of the discrepancies . The torsion is probably induced by the aerodynamic forces whose moments around the blade torsion axis must be large . These moments may come from 3D effects at the blade tip or from transonic effects , or they may be due to the flow separation from the blade upper surface on the retreating side of the rotor disk .

IV CONCLUSION

The computation of aerodynamic forces by means of integral methods is appealing to the dynamicist who must deal with very complex aeroelastic problems . The aerodynamic forces are decomposed into functions and the velocity induced by each function is computed . A condition of non separation of the flow from the blade surface is used to determine the aerodynamic forces . This approach is well suited when there is strong coupling between structure and aerodynamics because the induced velocities are only computed once . It can also be applied to stability problems . These methods were successfully used in airplane stability studies but their application to the helicopter rotor present many difficulties . The aerodynamic part of the problem is developed in this paper .

The helicopter blade is schematized by lifting lines. A new and accurate method for the treatment of the singularities which occur when a lifting line passes on a collocation point is given . The computer code has been validated by a comparison with a wind tunnel test . A more ambitious application to a flight test of the Gazelle helicopter has given acceptable results but has also brought to light some problems ; it is necessary to increase the number of lifting lines to compute the moments of the aerodynamic forces at the blade tip . A good prediction of the moments seems necessary in the case of the Gazelle rotor where large torsional deformations of the blades were measured . This study will be continued to include a full aeroelastic treatment of the problem .

REFERENCES

- 1 - DAT R , *Représentation d'une ligne portante animée d'un mouvement vibratoire par une ligne de doublets d'accélération* .La Recherche Aérospatiale N° 133 (1969) . English translation : NASA-TT-F-12952 (1970)
- 2 - Costes J-J , *Calcul des forces aérodynamiques instationnaires sur les pales d'un rotor d'hélicoptère* .AGARD REPORT N° 595 . English translation NASA-TT-F-15039 (1973) . See also : La Recherche Aérospatiale 1972-2 .
- 3 - Dat R , *La théorie de la surface portante appliquée à l'aile fixe et à l'hélice* . La Recherche Aérospatiale N° 1973-4 . English translation ESRO-TT-90 , (1974) .
- 4 - Dat R , Malfois J-P , *Sur le calcul du noyau de l'équation intégrale de la surface portante en écoulement subsonique instationnaire* . La Recherche Aérospatiale 1970-5
- 5 - Dat R , Akamatsu Y , *Représentation d'une aile par des lignes portantes ; application au calcul de l'interaction de deux ailes en tandem* .AGARD,Conf.Proc.N° 80 , Part. 1,n° 5 (1971) .
- 6 - Desmarais R.N , *An accurate and efficient method for evaluating the kernel of the integral equation relating pressure to normalwash in unsteady potential flow* . AIAA-82-0687

- 7 - Cunningham H.J , Desmarais R.N , *Generalization of the subsonic kernel function in the s-plane , with applications to flutter analysis* .NASA-TP-2292 March 1984
- 8 - Ando S , Kato M , *An improved kernel function computation in subsonic unsteady lifting surface theory* . Computer Methods in Applied Mechanics and Engineering Volume 49 , n° 3 ,June 1985
- 9 - Ando S , Ichikawa M , *A new numerical method of subsonic lifting surfaces - bis* . Transactions of the Japan Society for Aeronautical and Space Sciences Volume 29 , n° 84 ,1986
- 10- Forsythe G.E , Malcolm M.A , Moler C.B , *Computer methods for mathematical computations* . Prentice-Hall,Inc N.J. 07632 (1977) .
- 11 - Tran C.T , Desopper A , *An iteration technique coupling small perturbation transonic aerodynamic theory and rotor dynamics in forward flight* . To be presented at the 14th European Rotorcraft Forum . September 20-23 , 1988
- 12 - Costes J-J , *Introduction du décollément instationnaire dans la théorie du potentiel d'accélération . Application à l'hélicoptère* . La Recherche Aérospatiale 1975-3
- 13 - Costes J-J , *Rotor response prediction with nonlinear aerodynamic loads on the retreating blade* . 2 nd European Rotorcraft Forum 20-22 sept 1976 . Published in : Vertica vol 2 pp 73-85
- 14 - Yamauchi G.K , Heffernan R.M , Gaubert M , *Correlation of SA349/2 helicopter flight test data with a comprehensive rotorcraft model* . Presented at the Twelfth European Rotorcraft Forum , Garmisch-Partenkirchen W. Germany , sept. 1986.

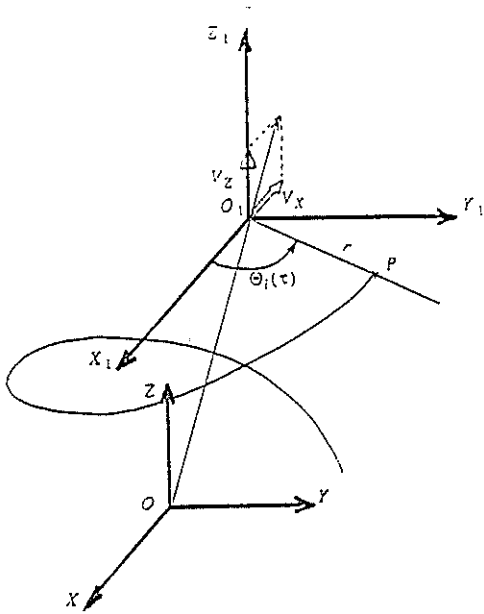


figure 1- Definition of the helicopter rotor
 OX,OY,OZ is an absolute reference frame .

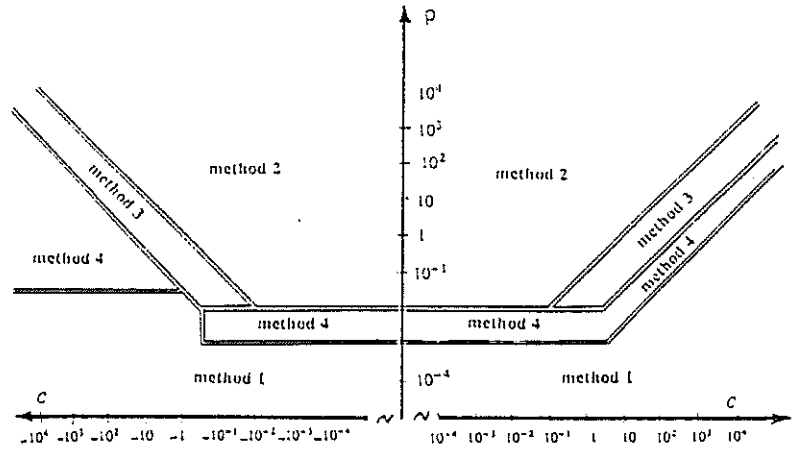
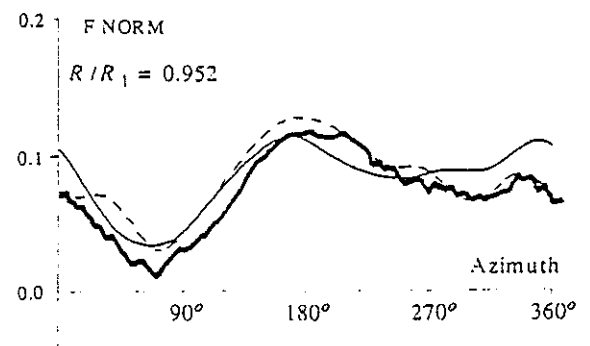
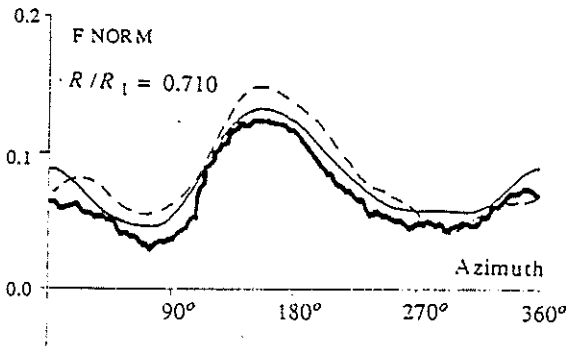
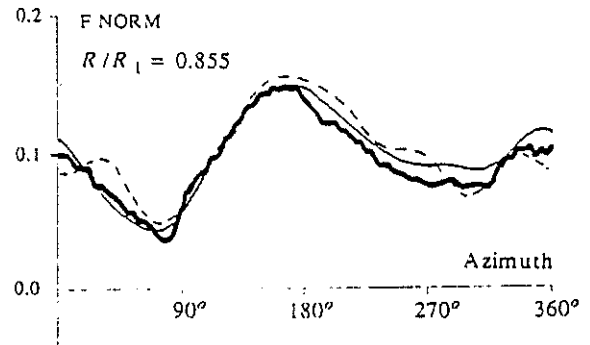
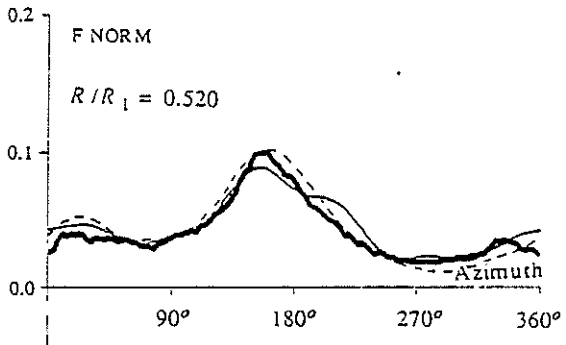
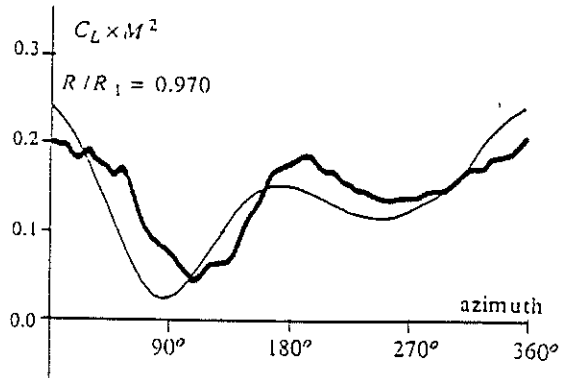
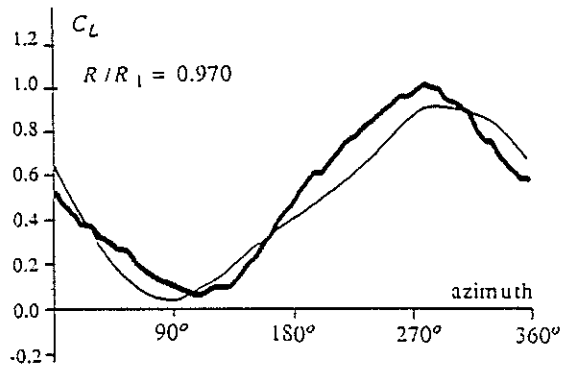
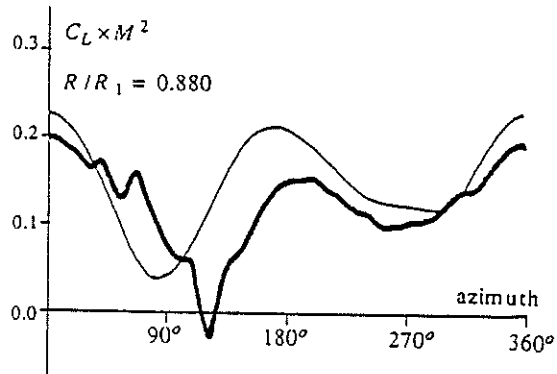
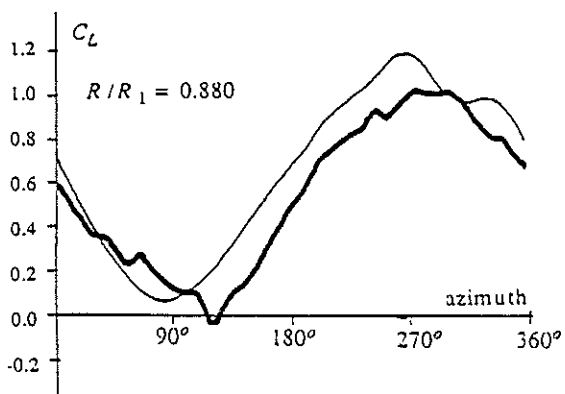
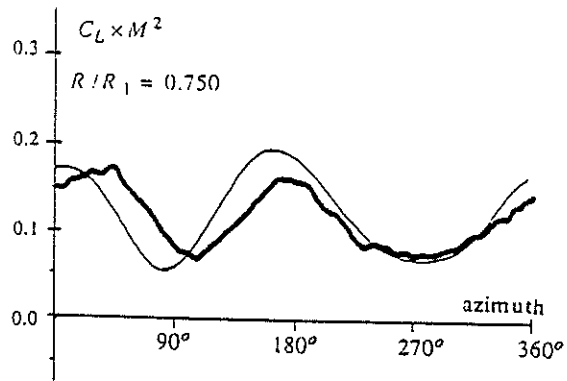
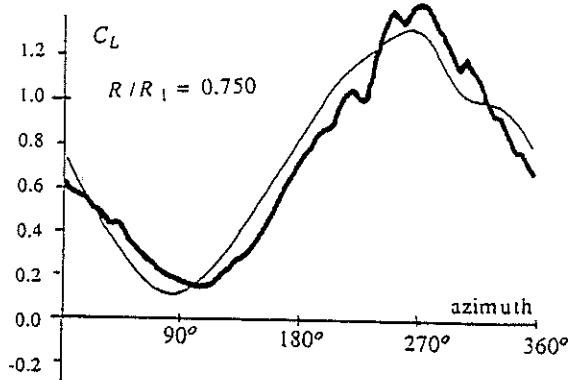


figure 2- The method used for the summation of the series S_1, S_2, S_3, S_4 depends from the values of the parameters ρ and c



- EXPERIMENT
- THEORY 1 lift. line corrected incomp. flow
- THEORY 1 lift. line compressible flow

figure 3- Comparison between theory and a wind tunnel test

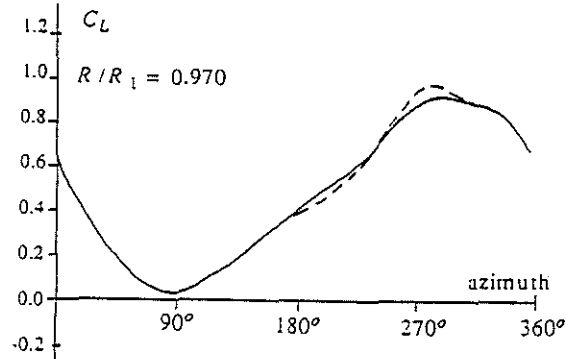
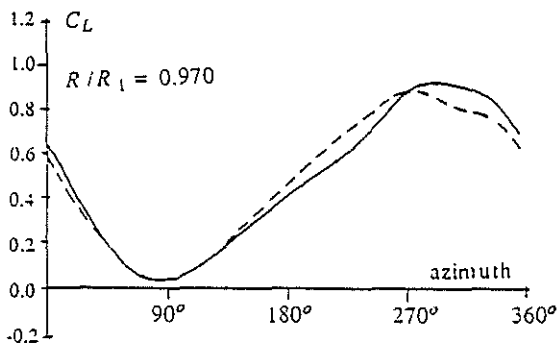
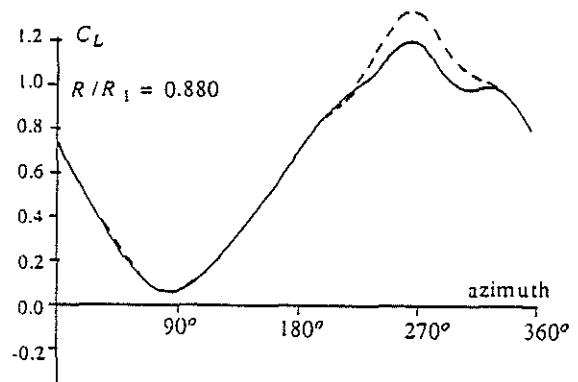
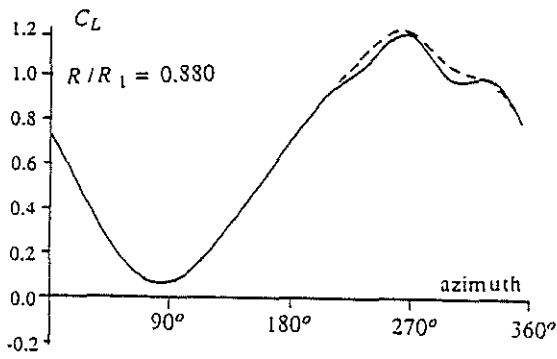
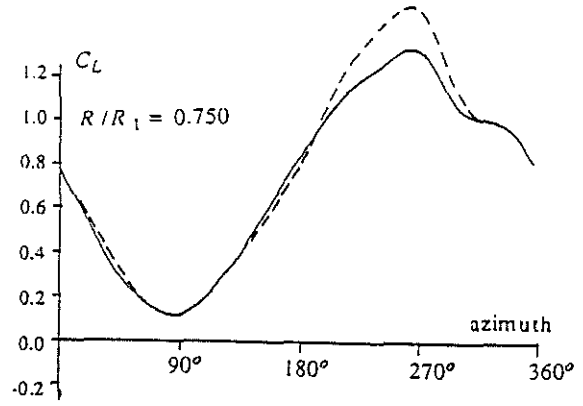
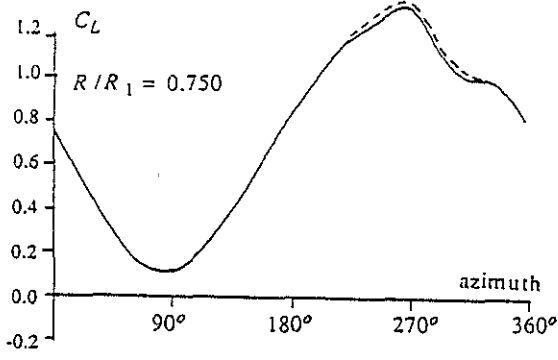


————— EXPERIMENT
 ————— THEORY | lifting line

————— EXPERIMENT
 ————— THEORY | lifting line

figure 4- Comparison between test and theory with a positioning of the collocation points to the leeward .

figure 5- Comparison between test and theory with a positioning of the collocation points to the leeward .



THEORY 1 lifting line leeward posit.
of coll. points
THEORY 1 lifting line fixed posit.
of coll. points

———— THEORY 1 lifting line
----- THEORY 2 lifting lines

figure 6- Comparison between results obtained with collocation points held fixed on the blade or with a positioning leeward .

figure 7- Comparison between results obtained with 1 and 2 lifting lines . For both computations there is a positioning of the collocation points to the leeward